ICCFD13-2026-180

Non-dissipative and robust KEEP (kinetic energy and entropy preserving) scheme for compressible two-phase flow seven-equation model

Soki Yoshida*, Shigetaka Kawai*, and Soshi Kawai*
Corresponding author: soki.yoshida@dc.tohoku.ac.jp
* Department of Aerospace Engineering, Graduate School of Engineering, Tohoku University, Japan.

Abstract: In order to accurately simulate compressible two-phase turbulent flows, non-dissipative properties are essential to resolve fine vortex structures without nonphysically smearing by numerical dissipation. However, the simulations of compressible two-phase flows with non-dissipative numerical schemes remain a major challenge, as steep interface gradients and high-density ratios trigger numerical instabilities in simulations of two-phase flows. To overcome this challenge, this paper proposed a novel non-dissipative and robust numerical scheme for compressible two-phase flows. We derive the kinetic energy and entropy preserving (KEEP) scheme, which exactly conserve the entropy, for compressible two-phase flows based on the seven-equation model. Our proposed scheme achieves both kinetic energy and entropy conservation at the discrete level and enables robust and non-dissipative simulations of compressible two-phase flows even under high-density ratio conditions, something that existing numerical schemes fail to do robustly. Furthermore, the proposed scheme is designed to satisfy the Interface equilibrium condition (IEC), and consistently coupled with the conservative phase-field method. The numerical tests verify the entropy-conservation property and satisfaction of IEC, and demonstrate the robustness of the proposed scheme for compressible two-phase turbulent flows even under realistic liquid-gas conditions.

Keywords: Compressible two-phase flows, Non-dissipative scheme, Entropy conservation.

1. Introduction

The numerical simulation of compressible two-phase flows is of great importance in various engineering applications, such as bubble acoustics, cavitation, atomization, and combustion. While the use of non-dissipative numerical schemes is crucial for high-fidelity simulations of such complex flows, the development of both robust and non-dissipative schemes for compressible two-phase flows remains a significant challenge. This difficulty arises from inherent numerical instabilities associated with compressible two-phase flows: the presence of steep gradients at the interface and high-density ratios between the two phases. To address this issue, this study proposes a novel non-dissipative and robust scheme for compressible two-phase flows. The key to constructing schemes that are both non-dissipative and robust is to satisfy secondary conservation properties—namely, conservation of kinetic energy and entropy—in addition to the primary conservation laws of mass, momentum, and total energy. In particular, for compressible flows, entropy conservation is crucial for suppressing nonphysical oscillations and numerical instabilities, as discussed by Tadmor [1]. Accordingly, various entropy conserving (EC) and entropy stable (ES) schemes have been proposed over the past years [2, 3, 4]. Among them, the kinetic energy and entropy preserving (KEEP) scheme proposed by Kuya et al. [5] stands out as a particularly significant contribution. The KEEP scheme is designed to simultaneously conserve kinetic energy and entropy at the discrete level, enabling robust and non-dissipative simulations of compressible single-phase turbulent flows.

In this study, we derive the KEEP scheme for compressible two-phase flows based on the seven-equation

model [6], which is the most general and complete models for compressible two-phase flows. We derive the forms of half-point numerical fluxes that strictly satisfy entropy conservation at the discrete level by analyzing the entropy conservation error. Furthermore, the proposed scheme is shown to satisfy the interface equilibrium condition (IEC), which is widely recognized as an essential property for two-phase flow simulations. Finally, the proposed KEEP scheme is consistently coupled with an interface-capturing method. In this study, the conservative phase-field method [7, 8, 9] is employed, and we propose the consistent discretizations of phase-field terms that satisfy kinetic energy and entropy conservation even in the presence of phase-field terms. The proposed scheme is validated through the numerical experiments for the one-dimensional (1D) volume fraction and density wave advection and for the three-dimensional (3D) inviscid two-phase Taylor–Green vortex. These numerical tests are conducted under realistic liquid-gas scenarios involving challenging high-density ratio conditions. It is demonstrated that the proposed KEEP achieves stable simulations of flows involving such severe conditions without adding numerical dissipation, something that existing schemes fail to do robustly. Further details of the present study are provided in Ref. [10].

2. Governing Equations

Seven-equation model is the most general model, allowing for non-equilibrium of both velocity and pressure between the two phases. This was first proposed by Baer and Nunziato [6] and later improved in several studies [11, 12]. The full model formulation and detailed description of seven-equation model can be found in [13]. For simplicity, the governing equations are presented in their one-dimensional form. The volume fraction advection equation is given by

$$\frac{\partial \phi_1}{\partial t} + u_I \frac{\partial \phi_1}{\partial x} = \mu(p_1 - p_2), \tag{1}$$

and the conservation equations of mass, momentum, and total energy for each phase are

$$\frac{\partial \phi_k \rho_k}{\partial t} + \frac{\partial \phi_k \rho_k u_k}{\partial x} = 0, \tag{2}$$

$$\frac{\partial \phi_k \rho_k u_k}{\partial t} + \frac{\partial \phi_k \rho_k u_k u_k}{\partial x} + \frac{\partial \phi_k p_k}{\partial x} = p_I \frac{\partial \phi_k}{\partial x} + \lambda(u_{k*} - u_k), \tag{3}$$

$$\frac{\partial \phi_k \rho_k E_k}{\partial t} + \frac{\partial \phi_k \rho_k e_k u_k}{\partial x} + \frac{\partial \phi_k \rho_k \kappa_k u_k}{\partial x} + \frac{\partial \phi_k p_k u_k}{\partial x} = p_I u_I \frac{\partial \phi_k}{\partial x} - \mu p'_I(p_k - p_{k*}) + \lambda u'_I(u_{k*} - u_k). \tag{4}$$

Here, ϕ_k, ρ_k, u_k, E_k, and p_k are the volume fraction, density, velocity, total energy per unit mass, and pressure of phase k ($k = 1, 2$). $k*$ denotes the conjugate phase to k; i.e., $k = 1$ implies $k* = 2$, and vice versa. The volume fraction of each phase satisfies the saturation condition $\phi_1 + \phi_2 = 1$. The total energy per unit mass is defined as $E_k = e_k + \kappa_k$, where e_k and κ_k are the internal energy and kinetic energy per unit mass of phase k. The subscript I denotes quantities at the interfaces, including the interface velocity, u_I, and the interface pressure, p_I. In this work, we employ the model proposed by Saurel et al. [12], which is written as

$$\begin{aligned} u_I &= u'_I + \operatorname{sgn}\left(\frac{\partial \phi_1}{\partial x}\right) \frac{p_2 - p_1}{Z_1 + Z_2}, \\ p_I &= p'_I + \frac{Z_1 Z_2}{Z_1 + Z_2} \operatorname{sgn}\left(\frac{\partial \phi_1}{\partial x}\right)(u_2 - u_1), \end{aligned} \tag{5}$$

where

$$u'_I = \frac{Z_1 u_1 + Z_2 u_2}{Z_1 + Z_2}, \; p'_I = \frac{Z_1 p_2 + Z_2 p_1}{Z_1 + Z_2}. \tag{6}$$

Here, $Z_k = \rho_k c_k$ is the acoustic impedance of phase k, and c_k is the speed of sound of phase k. Although Eqs. (5) and (6) are adopted in this study, the other options are equally applicable (e.g.,[6, 11]). The non-equilibrium source terms on the right hand side of Eqs. (1)–(4) represent the relaxation effect of velocity and pressure between the two phases. λ and μ are the rates at which the velocity and pressure of each phase relax toward mechanical equilibrium, respectively. These relaxation processes are assumed to occur instantaneously to impose the interface jump conditions, i.e., $\lambda \to \infty$ and $\mu \to \infty$. Following the operator splitting approach [11], these relaxation terms are treated separately from the hyperbolic part of the governing equation. The hyperbolic part of the governing equation is

$$\frac{\partial \phi_1}{\partial t} + u_I \frac{\partial \phi_1}{\partial x} = 0, \tag{7}$$

$$\frac{\partial \phi_k \rho_k}{\partial t} + \frac{\partial \phi_k \rho_k u_k}{\partial x} = 0, \tag{8}$$

$$\frac{\partial \phi_k \rho_k u_k}{\partial t} + \frac{\partial \phi_k \rho_k u_k u_k}{\partial x} + \frac{\partial \phi_k p_k}{\partial x} = p_I \frac{\partial \phi_k}{\partial x}, \tag{9}$$

$$\frac{\partial \phi_k \rho_k E_k}{\partial t} + \frac{\partial \phi_k \rho_k e_k u_k}{\partial x} + \frac{\partial \phi_k \rho_k \kappa_k u_k}{\partial x} + \frac{\partial \phi_k p_k u_k}{\partial x} = p_I u_I \frac{\partial \phi_k}{\partial x}. \tag{10}$$

For the relaxation solver, the simple analytical approach described in [14] is adopted in this study. The full seven-equation model (Eqs. (1)–(4)) yields the following entropy equation:

$$\begin{aligned}\frac{\partial \phi_k \rho_k s_k}{\partial t} + \frac{\partial \phi_k \rho_k s_k u_k}{\partial x} = \frac{1}{T_k}\Big[&(p_I - p_k)(u_I - u_k)\frac{\partial \phi_k}{\partial x} + \mu(p'_I - p_k)(p_{k*} - p_k) \\ &+ \lambda(u'_I - u_k)(u_{k*} - u_k)\Big],\end{aligned} \tag{11}$$

where the s_k and T_k are the specific entropy and temperature of phase k, respectively. Focusing the hyperbolic part, this equation reduces to

$$\frac{\partial \phi_k \rho_k s_k}{\partial t} + \frac{\partial \phi_k \rho_k s_k u_k}{\partial x} = \frac{1}{T_k}\Big[(p_I - p_k)(u_I - u_k)\frac{\partial \phi_k}{\partial x}\Big]. \tag{12}$$

The term on the right-hand side is non-negative with the interfacial parameters in Eq. (5), which is consistent with the second law of thermodynamics.

For the equation of state (EoS), the stiffened-gas EoS is employed in this study. The internal energy of each phase k, e_k, can be expressed as a function of density and pressure, $e_k = e_k(\rho_k, p_k)$, or, equivalently, as a function of density and temperature, $e_k = e_k(\rho_k, T_k)$, and is given by

$$e_k = \frac{p_k + \gamma_k \pi_{\infty,k}}{(\gamma_k - 1)\rho_k} = C_{v,k} T_k + \frac{\pi_{\infty,k}}{\rho_k}. \tag{13}$$

$\gamma_k = C_{p,k}/C_{v,k}$ is the ratio of specific heats of phase k and $\pi_{\infty,k}$ is the reference pressure. Also, the speed of sound c_k, the specific enthalpy h_k and entropy s_k are defined as

$$c_k = \sqrt{\gamma_k \frac{p_k + \pi_{\infty,k}}{\rho_k}}, \tag{14}$$

$$h_k = C_{v,k} \gamma_k T_k, \tag{15}$$

$$s_k = C_{v,k} \log T_k - C_{v,k}(\gamma_k - 1) \log \rho_k. \tag{16}$$

3. Formulation of proposed scheme

In this section, we briefly describe the formulation of the proposed scheme; further details can be found in Ref. [10]. Our proposed scheme achieves both non-dissipative and robust properties by satisfying the following three properties:

- **Kinetic energy and entropy conservation.**
  The main contribution of this work is the derivation of a discretization that satisfies the discrete conservation of the secondary quantities: kinetic energy and entropy. This property has been shown to substantially enhance the robustness of numerical schemes, particularly for single-phase flows [1, 2, 4]. While several works [15, 16] attempted to construct numerical schemes that satisfy this property for compressible two-phase flow, their formulation failed to satisfy the exact entropy conservation. As will be demonstrated in the numerical experiments, satisfying strict entropy conservation is crucial for the numerical stability of two-phase flow simulations with high-density ratios.

- **Interface equilibrium conditions (IEC).**
  The IEC denotes the requirement that initially uniform pressure and velocity fields across the interface be preserved throughout the numerical time evolution. Violating the IEC can lead to spurious oscillations at the interface, which can cause numerical instability [17].

- **Consistent coupling with interface-capturing methods.**
  In order to handle the sharp interface profile with non-dissipative numerical schemes, the proposed scheme has to be coupled with an interface-capturing method. The conservative formulation of the phase-field method [9, 7, 8] is employed in this study, which is designed to satisfy the boundedness of the volume fraction ϕ_1 between 0 and 1. We propose consistent discretizations of the phase terms so that kinetic energy conservation, entropy conservation, and the IEC are retained even in the presence of phase-field terms.

3.1 Kinetic energy and entropy conservation

The main focus of this work is to derive a spatial discretization of hyperbolic part of the governing equations (Eqs. (7)–(10)) that satisfies the discrete conservation of kinetic energy and entropy. We denote the spatial discretization as

$$\left.\frac{\partial f}{\partial x}\right|_m \simeq D|_m(f) \equiv \frac{\widetilde{f}|_{m+\frac{1}{2}} - \widetilde{f}|_{m-\frac{1}{2}}}{\Delta x}. \tag{17}$$

The $D|_m$ represents a discrete spatial differential operator at the cell m, $\widetilde{f}|_{m\pm\frac{1}{2}}$ is the numerical half-point flux at the cell interface $m\pm\frac{1}{2}$, and Δx is the grid spacing. Following this notation, the spatial discretization of Eqs. (7)–(10) can be written as

$$\left.\frac{\partial \phi_k}{\partial t}\right|_m = -\,u_I|_m D|_m\left(\phi_k\right), \tag{18}$$

$$\left.\frac{\partial \phi_k \rho_k}{\partial t}\right|_m = -\,D|_m\left(\phi_k \rho_k u_k\right), \tag{19}$$

$$\left.\frac{\partial \phi_k \rho_k u_k}{\partial t}\right|_m = -\,D|_m\left(\phi_k \rho_k u_k u_k\right) - D|_m\left(\phi_k p_k\right) + p_I|_m D|_m\left(\phi_k\right), \tag{20}$$

$$\left.\frac{\partial \phi_k \rho_k E_k}{\partial t}\right|_m = -\,D|_m\left(\phi_k \rho_k e_k u_k\right) - D|_m\left(\phi_k \rho_k \kappa_k u_k\right) - D|_m\left(\phi_k p_k u_k\right) + p_I|_m u_I|_m D|_m\left(\phi_k\right). \tag{21}$$

We first extend the formulation of the KEEP scheme for single-phase flows, originally proposed by Kuya et al. [5], in a straightforward manner, which serves as the baseline for the proposed discretization.

Following their approach, some of the numerical fluxes in Eqs. (18)–(21) can be determined as

$$\widetilde{\phi_k\rho_k u_k u_k}|_{m\pm\frac{1}{2}} = \widetilde{\phi_k\rho_k u_k}|_{m\pm\frac{1}{2}}\overline{u_k}|_{m\pm\frac{1}{2}}, \tag{22}$$

$$\widetilde{\phi_k\rho_k \kappa_k u_k}|_{m\pm\frac{1}{2}} = \widetilde{\phi_k\rho_k u_k}|_{m\pm\frac{1}{2}}\frac{u_k|_m u_k|_{m\pm1}}{2}, \tag{23}$$

$$\widetilde{\phi_k p_k}|_{m\pm\frac{1}{2}} = \overline{\phi_k p_k}|_{m\pm\frac{1}{2}}, \tag{24}$$

$$\widetilde{\phi_k p_k u_k}|_{m\pm\frac{1}{2}} = \frac{u_k|_m(\phi_k p_k)|_{m\pm1} + u_k|_{m+1}(\phi_k p_k)|_m}{2}, \tag{25}$$

where $\overline{\psi}|_{m\pm\frac{1}{2}}$ represents arithmetic mean $(\psi|_m + \psi|_{m\pm1})/2$. This formulation ensures the kinetic energy conservation at the discrete level and the correct representation of the energy exchange between kinetic and internal energy.

In Eq. (18)-(21), the numerical half-point fluxes $\widetilde{\phi_k\rho_k u_k}|_{m\pm\frac{1}{2}}$, $\widetilde{\phi_k\rho_k e_k u_k}|_{m\pm\frac{1}{2}}$, $\widetilde{\phi_k}|_{m\pm\frac{1}{2}}$ and $\widetilde{u_k}|_{m\pm\frac{1}{2}}$ have not yet been specified, and they are determined to satisfy the discrete entropy conservation. To derive entropy-conserving numerical fluxes, the theoretical analysis of the entropy conservation error [18] is performed on the discretized governing equations (Eqs. (18)–(21)). The detail of the derivation of the entropy-conserving numerical fluxes is described in Ref. [10], and the final formulation is given by

$$\widetilde{\phi_k}|_{m\pm\frac{1}{2}} = \overline{\phi}|_{m\pm\frac{1}{2}}, \tag{26}$$

$$\widetilde{u_k}|_{m+\frac{1}{2}} = \overline{u_k}|_{m+\frac{1}{2}}, \tag{27}$$

$$\widetilde{\phi_k\rho_k u_k}|_{m\pm\frac{1}{2}} = \overline{\rho_k}|^{\log}_{m\pm\frac{1}{2}}\widetilde{\phi_k u_k}|_{m\pm\frac{1}{2}}, \tag{28}$$

$$\widetilde{\phi_k\rho_k e_k u_k}|_{m\pm\frac{1}{2}} = \left(C_{v,k}\left(\overline{(1/T_k)}|^{\log}_{m\pm\frac{1}{2}}\right)^{-1} + \frac{\pi_{\infty,k}}{\overline{\rho_k}|^{\log}_{m\pm\frac{1}{2}}}\right)\widetilde{\phi_k\rho_k u_k}|_{m\pm\frac{1}{2}}, \tag{29}$$

where

$$\widetilde{\phi_k u_k}|_{m\pm\frac{1}{2}} = \frac{\phi_k|_m u_k|_{m\pm1} + \phi_k|_{m\pm1} u_k|_m}{2}. \tag{30}$$

It is worth noting that the flux $\widetilde{\phi_k u_k}|_{m\pm\frac{1}{2}}$ does not appear explicitly in the seven equation model; it is introduced solely through the entropy-conserving mass advection flux $\widetilde{\phi_k\rho_k u_k}|_{m+\frac{1}{2}}$ defined above.

$\overline{\psi}|^{\log}_{m\pm\frac{1}{2}}$ denotes the logarithmic mean defined as

$$\overline{\psi}|^{\log}_{m\pm\frac{1}{2}} = \begin{cases} \psi|_m, & \text{if } \psi|_m = \psi|_{m\pm1} \\ \dfrac{\psi|_{m\pm1} - \psi|_m}{\log\psi|_{m\pm1} - \log\psi|_m}. & \text{else} \end{cases} \tag{31}$$

Although these numerical fluxes in Eqs. (28) and (29) satisfy the exact entropy conservation, the direct implementation of the logarithmic mean can be problematic because they involve logarithmic mean. In particular, the evaluation of the logarithmic mean requires an ad hoc local treatment to avoid division by zero, which increases the computational cost. Furthermore, as discussed in Ref. [10], the computation of the logarithmic mean is susceptible to round-off errors, which may potentially lead to numerical instability for the compressible two-phase flow simulations. To address this issue, the logarithmic mean has often been approximated using other mean values [19, 20]. Notably, Kawai & Kawai [20] demonstrated that the geometric mean is the best approximation of the logarithmic mean, and this argument can be straightforwardly extended to our proposed framework. A detailed discussion and derivation are left to

Ref. [10]; in this study, we propose the following geometric-mean-based approximation:

$$\widetilde{\phi_k\rho_k u_k}|_{m\pm\frac{1}{2}} = \overline{\rho_k}|^{\mathrm{geo}}_{m\pm\frac{1}{2}} \left(1 - \frac{1}{6}(\Delta\rho_k|_{m\pm\frac{1}{2}})^2\right)^{-1} \widetilde{\phi_k u_k}|_{m\pm\frac{1}{2}}, \tag{32}$$

$$\widetilde{\phi_k\rho_k e_k u_k}|_{m\pm\frac{1}{2}} = \left[C_{v,k}\overline{T_k}|^{\mathrm{geo}}_{m\pm\frac{1}{2}} \left(1 - \frac{1}{6}(\Delta T_k|_{m\pm\frac{1}{2}})^2\right) + \frac{\pi_{\infty,k}}{\overline{\rho_k}|^{\mathrm{geo}}_{m\pm\frac{1}{2}}} \left(1 - \frac{1}{6}(\Delta T_k|_{m\pm\frac{1}{2}})^2\right)\right] \widetilde{\rho_k\phi_k u_k}|_{m\pm\frac{1}{2}}, \tag{33}$$

where $\overline{\psi}|^{\mathrm{geo}}_{m\pm\frac{1}{2}}$ denotes the geometric mean $\sqrt{\psi|_m\psi|_{m\pm1}}$, and $\Delta\psi|_{m\pm\frac{1}{2}}$ is defined as

$$\Delta\psi|_{m\pm\frac{1}{2}} = \pm\frac{\psi|_{m\pm1} - \psi|_m}{2\overline{\psi}|_{m\pm\frac{1}{2}}}. \tag{34}$$

3.2 Interface equilibrium condition (IEC)

Here, we confirm that the proposed formulation (Eqs. (22)–(27), (32) and (33)) satisfies the IEC, which is defined as

$$\left.\frac{\partial u_k}{\partial t}\right|_m = 0, \quad \left.\frac{\partial p_k}{\partial t}\right|_m = 0, \quad (k = \{1,2\},\ \forall m) \quad \text{if } \begin{cases} u_1|_m = u_2|_m = u_I|_m = u_0, \\ p_1|_m = p_2|_m = p_I|_m = p_0. \end{cases} \tag{35}$$

For the velocity, the time-evolution equation is derived as

$$\frac{\partial u_k}{\partial t} = \frac{1}{\phi_k\rho_k}\left(\frac{\partial\phi_k\rho_k u_k}{\partial t} - u_k\frac{\partial\phi_k\rho_k}{\partial t}\right). \tag{36}$$

Substituting Eq. (19) and (20) leads to

$$\left.\frac{\partial u_k}{\partial t}\right|_m = -\frac{1}{\phi_k\rho_k}(D|_m(\phi_k\rho_k u_k u_k) + D|_m(\phi_k p_k) - p_I|_m D|_m(\phi_k) - u_k D|_m(\phi_k\rho_k u_k)). \tag{37}$$

If the proposed fluxes are substituted into the above equation,

$$\begin{aligned}\left.\frac{\partial u_k}{\partial t}\right|_m = -\frac{1}{\phi_k\rho_k}\Bigg(&\frac{\widetilde{\phi_k\rho_k u_k}|_{m+\frac{1}{2}}\overline{u_k}|_{m+\frac{1}{2}} - \widetilde{\phi_k\rho_k u_k}|_{m-\frac{1}{2}}\overline{u_k}|_{m-\frac{1}{2}}}{\Delta x} + \frac{\overline{\phi_k p_k}|_{m+\frac{1}{2}} - \overline{\phi_k p_k}|_{m-\frac{1}{2}}}{\Delta x} \\ &- p_I|_m\frac{\overline{\phi_k}|_{m+\frac{1}{2}} - \overline{\phi_k}|_{m-\frac{1}{2}}}{\Delta x} - u_k|_m\frac{\widetilde{\phi_k\rho_k u_k}|_{m+\frac{1}{2}} - \widetilde{\phi_k\rho_k u_k}|_{m-\frac{1}{2}}}{\Delta x}\Bigg).\end{aligned} \tag{38}$$

Given the uniform velocity and pressure fields, the right-hand side of the above equation vanishes, demonstrating that the proposed numerical fluxes are consistent with the IEC in terms of velocity.

The time-evolution equation of pressure is given by

$$\frac{\partial p_k}{\partial t} = \frac{\gamma_k - 1}{\phi_k}\left(\frac{\partial\phi_k\rho_k E_k}{\partial t} - u_k\frac{\partial\phi_k\rho_k u_k}{\partial t} + \frac{u_k^2}{2}\frac{\partial\phi_k\rho_k}{\partial t} - \frac{p_k + \gamma_k\pi_{\infty,k}}{\gamma_k - 1}\frac{\partial\phi_k}{\partial t}\right). \tag{39}$$

Substituting the discretized governing equations (Eqs (18)–(21)) yields

$$\begin{aligned}\left.\frac{\partial p_k}{\partial t}\right|_m = -\frac{\gamma_k - 1}{\phi_k}\Bigg(& D|_m\left(\phi_k\rho_k e_k u_k\right) - \frac{p_k|_m + \gamma_k\pi_{\infty,k}}{\gamma_k - 1}u_I|_m D|_m(\phi_k) \\ & + D|_m\left(\phi_k\rho_k\kappa_k u_k\right) - u_k|_m D|_m\left(\phi_k\rho_k u_k u_k\right) + \frac{u_k|_m^2}{2}D|_m\left(\phi_k\rho_k u_k\right) \\ & + D|_m\left(\phi_k p_k u_k\right) - u_k|_m D|_m\left(\phi_k p_k\right) \\ & - p_I|_m u_I|_m D|_m\left(\phi_k\right) + u_k|_m p_I|_m D|_m\left(\phi_k\right)\Bigg).\end{aligned} \tag{40}$$

Substituting the proposed numerical fluxes and assuming the uniform velocity and pressure fields, this reduces to

$$\frac{\partial p_k}{\partial t} = -\frac{\gamma_k - 1}{\phi_k}\left(\frac{\widetilde{\phi_k\rho_k e_k}u_k|_{m+\frac{1}{2}} - \widetilde{\phi_k\rho_k e_k}u_k|_{m-\frac{1}{2}}}{\Delta x} - \frac{p_0 + \gamma_k\pi_{\infty,k}}{\gamma_k - 1}u_0|_m\frac{\overline{\phi_k}|_{m+\frac{1}{2}} - \overline{\phi_k}|_{m-\frac{1}{2}}}{\Delta x}\right). \tag{41}$$

Hence, to satisfy the IEC in terms of pressure, the following condition should be satisfied:

$$\widetilde{\phi_k\rho_k e_k}u_k|_{m\pm\frac{1}{2}} = \frac{p_0 + \gamma_k\pi_{\infty,k}}{\gamma_k - 1}u_0\overline{\phi_k}|_{m\pm\frac{1}{2}}. \tag{42}$$

The proposed internal energy flux (Eq. (33)) satisfies this equation under the uniform pressure and velocity fields. Therefore, the proposed numerical fluxes satisfy the IEC in terms of both velocity and pressure.

Conversely, there are various formulations that fail to satisfy the IEC. As discussed in [21], the following simple approximation of Eqs. (28) and (29) violates the IEC:

$$\widetilde{\phi_k\rho_k u_k}|_{m\pm\frac{1}{2}} = \overline{\rho_k}|_{m\pm\frac{1}{2}}\widetilde{\phi_k u_k}|_{m\pm\frac{1}{2}}, \tag{43}$$

$$\begin{aligned}\widetilde{\phi_k\rho_k e_k}u_k|_{m\pm\frac{1}{2}} &= \overline{\rho_k}|_{m\pm\frac{1}{2}}\overline{e_k}|_{m\pm\frac{1}{2}}\widetilde{\phi_k u_k}|_{m\pm\frac{1}{2}} \\ &= \left(C_{v,k}\overline{T_k}|_{m\pm\frac{1}{2}} + \frac{\pi_{\infty,k}}{\overline{\rho_k}|^{\mathrm{har}}_{m\pm\frac{1}{2}}}\right)\widetilde{\phi_k\rho_k u_k}|_{m\pm\frac{1}{2}},\end{aligned} \tag{44}$$

where $\overline{\psi}|^{\mathrm{har}}_{m+\frac{1}{2}}$ denotes harmonic mean $2\psi|_m\psi|_{m+1}/(\psi|_m + \psi|_{m+1})$. On the other hand, Hatashita & Jain [16] employ the following formulation analogous to the numerical fluxes for single-phase flows in [21] as

$$\widetilde{\phi_k\rho_k u_k}|_{m\pm\frac{1}{2}} = \overline{\phi_k\rho_k}|_{m\pm\frac{1}{2}}\overline{u_k}|_{m\pm\frac{1}{2}}, \tag{45}$$

$$\widetilde{\phi_k\rho_k e_k}u_k|_{m\pm\frac{1}{2}} = \overline{\phi_k\rho_k e_k}|_{m\pm\frac{1}{2}}\overline{u_k}|_{m\pm\frac{1}{2}}. \tag{46}$$

It is also worth noting that Jain and Moin [15] employed a similar formulation, although these approaches sacrifice the entropy conservation property to prioritize consistency with the IEC.

3.3 Consistent coupling with interface-capturing methods

Here, the consistent coupling of the proposed scheme with the interface-capturing method is briefly described. We employ the conservative phase-field which is originally applied to incompressible flows [7, 8], and later extended to the compressible two-phase flow in [9, 15, 16]. The analytically consistent formulation of the hyperbolic part of the governing equations (Eqs. (7)–(10)) with the phase-field terms

is given by

$$\frac{\partial \phi_1}{\partial t} + u_I \frac{\partial \phi_1}{\partial x} = \frac{\partial a_1}{\partial x}, \tag{47}$$

$$\frac{\partial \phi_k \rho_k}{\partial t} + \frac{\partial \phi_k \rho_k u_k}{\partial x} = \frac{\partial a_k \rho_k}{\partial x}, \tag{48}$$

$$\frac{\partial \phi_k \rho_k u_k}{\partial t} + \frac{\partial \phi_k \rho_k u_k u_k}{\partial x} + \frac{\partial \phi_k p_k}{\partial x} = p_I \frac{\partial \phi_k}{\partial x} + \frac{\partial a_k \rho_k u_k}{\partial x}, \tag{49}$$

$$\frac{\partial \phi_k \rho_k E_k}{\partial t} + \frac{\partial \phi_k \rho_k e_k u_k}{\partial x} + \frac{\partial \phi_k \rho_k \kappa_k u_k}{\partial x} + \frac{\partial \phi_k p_k u_k}{\partial x} = p_I u_I \frac{\partial \phi_k}{\partial x} + \frac{\partial a_k \rho_k e_k}{\partial x} + \frac{\partial a_k \rho_k \kappa_k}{\partial x}, \tag{50}$$

where a_k is the interface regularization flux of phase k, defined as

$$a_k = \Gamma \left[\epsilon \left(\frac{\partial \phi_k}{\partial x} \right) - (\phi_k - \phi_{\min})(1 - \phi_k - \phi_{\min}) n_k \right]. \tag{51}$$

Here, n_k is the normal vector of the interface, and $\phi_{\min}$ is the parameter that determines the volume fraction floor and ceiling. As discussed in [8, 9], the parameters Γ and ϵ must be chosen so as to maintain the boundedness of the volume fraction field.

This formulation admits the analytical kinetic energy and entropy equation in the following form:

$$\frac{\partial \phi_k \rho_k \kappa_k}{\partial t} = -\frac{\partial \phi_k \rho_k \kappa_k u_k}{\partial x} - u_k \frac{\partial \phi_k p_k}{\partial x} + p_I u_k \frac{\partial \phi_k}{\partial x} + \frac{\partial a_k \rho_k \kappa_k}{\partial x}. \tag{52}$$

$$\frac{\partial \phi_k \rho_k s_k}{\partial t} = -\frac{\partial \phi_k \rho_k s_k u_k}{\partial x} + \frac{1}{T_k}(p_I - p_k)(u_I - u_k) \frac{\partial \phi_k}{\partial x} + \frac{\partial a_k \rho_k s_k}{\partial x}. \tag{53}$$

The last terms of each equation represent the effect of the interface regularization on the kinetic energy and entropy. These terms are expressed in conservative form, which analytically ensures kinetic energy and entropy conservation even in the presence of the phase-field terms.

In this study, we proposed to discretize the phase-field terms to conserve kinetic energy and entropy at the discrete level in the same manner as the convective fluxes:

$$\widetilde{a_k \rho_k u_k}|_{m\pm\frac{1}{2}} = \widetilde{a_k \rho_k}|_{m\pm\frac{1}{2}} \overline{u_k}|_{m\pm\frac{1}{2}}, \tag{54}$$

$$\widetilde{a_k \rho_k \kappa_k}|_{m\pm\frac{1}{2}} = \widetilde{a_k \rho_k}|_{m\pm\frac{1}{2}} \frac{u_k|_m u_k|_{m\pm1}}{2}. \tag{55}$$

$$\widetilde{a_k \rho_k}|_{m\pm\frac{1}{2}} = \overline{\rho_k}|^{\text{geo}}_{m\pm\frac{1}{2}} \left(1 - \frac{1}{6}(\Delta \rho_k|_{m\pm\frac{1}{2}})^2 \right)^{-1} \widetilde{a_k}|_{m\pm\frac{1}{2}}, \tag{56}$$

$$\widetilde{a_k \rho_k e_k}|_{m\pm\frac{1}{2}} = \left[C_{v,k} \overline{T_k}|^{\text{geo}}_{m\pm\frac{1}{2}} \left(1 - \frac{1}{6}(\Delta T_k|_{m\pm\frac{1}{2}})^2 \right) + \frac{\pi_{\infty,k}}{\overline{\rho_k}|^{\text{geo}}_{m\pm\frac{1}{2}}} \left(1 - \frac{1}{6}(\Delta T_k|_{m\pm\frac{1}{2}})^2 \right) \right] \widetilde{a_k \rho_k}|_{m\pm\frac{1}{2}}. \tag{57}$$

$$\tag{58}$$

It should be noted that the IEC can be shown to hold in the presence of phase-field terms by using a straightforward argument analogous to that presented in Section 3.2.

4. Numerical experiments

In this section, numerical experiments are presented for one-dimensional (1D) volume-fraction and density-wave advection and the three-dimensional (3D) inviscid two-phase Taylor–Green vortex. We compare three different formulations:

- Proposed (Eqs. (32) and (33))
  The geometric-mean-based approximation of Eqs. (28) and (29), and it satisfies the IEC.
- NIE (Eqs. (43) and (44))
  Although it serves as a simple approximation of Eqs. (28) and (29), it violates the IEC.
- IE-H (Eqs. (45) and (46))
  The formulation employed by Hatashita & Jain [16] for satisfying the IEC.

The other numerical fluxes are defined by Eqs. (22)–(27) for all formulations.

In all cases, the physical properties of each phase are assumed to be those of air and water, and the parameters are chosen to be $\rho_{01} = 1000$, $\rho_{02} = 1$, $\gamma_1 = 4.4$, $\gamma_2 = 1.4$, $\pi_{\infty,1} = 6000$, and $\pi_{\infty,2} = 0$. This simulation conditions are designed to be challenging and prone to instability by employing realistic parameters for gas and liquid, which feature a high-density ratio. Throughout this work, the four stage Runge–Kutta (RK4) method is used for the time integration, and the temporal discretization errors are assumed to be negligibly small compared to those of the spatial discretization. The time-step size is determined by the Courant-Friedrichs-Lewy (CFL) condition, based on the maximum speed of sound and the maximum velocity of the two phases.

4.1 1D volume fraction and density wave advection

This test is conducted to verify that the proposed scheme satisfies both the entropy conservation and the IEC at the discrete level. The initial conditions are set:

$$\begin{aligned}
\phi_1 &= 0.5 + 0.4 \sin\left(2\pi x + 0.5\pi\right), \\
\rho_1 &= \rho_{01} + 0.1 \times \rho_{01} \sin(2\pi x), \\
\rho_2 &= \rho_{02} + 0.1 \times \rho_{02} \sin(2\pi x), \\
u_1 &= u_2 = u_0 = 1.0, \\
p_1 &= p_2 = p_0 = 0.9.
\end{aligned} \tag{59}$$

The computational domain is set to $x \in [0, 1]$ with periodic boundary conditions, and the number of equidistant grid points is set to 100. The CFL number is set to approximately 0.05 for the time integration. In this case, the velocity and pressure relaxation step is skipped, and only the hyperbolic part without the phase-field terms (Eqs. (7)–(10)) is solved. If the initial uniform velocity and pressure field is maintained, Eq.(12) reduces to

$$\frac{\partial \phi_k \rho_k s_k}{\partial t} + \frac{\partial \phi_k \rho_k s_k u_k}{\partial x} = 0, \tag{60}$$

which ensures that entropy is analytically conserved.

Figure 1a shows the time histories of the conservation error of the total entropy $\rho s = \phi_1 \rho_1 s_1 + \phi_2 \rho_2 s_2$ averaged over the domain. $\rho_0 s_0$ represents the initial total entropy. It is seen that the Proposed scheme satisfies the entropy conservation at the discrete level, whereas the other two schemes fail during the computation. In particular, although NIE shows relatively good entropy conservation property, it diverges at $t \approx 65$ due to the violation of the IEC. IE-H blow up $t \approx 32$ due to the accumulation of the entropy conservation error. In addition, the instantaneous pressure error distributions after one flow-though time are presented in Figure 1b and 1c. As expected, the proposed scheme and IE-H maintain the IEC at the discrete level, whereas NIE produces spurious pressure oscillations.

4.2 3D inviscid two-phase Taylor–Green vortex

The inviscid 3D Taylor–Green vortex is useful test case to investigate the robustness of numerical schemes. Although this test case was extended to compressible two-phase flows by Jain and Moin [15], they assumed

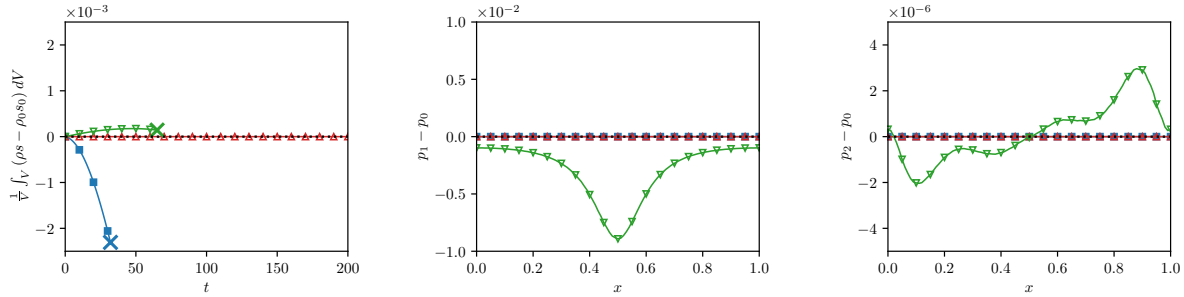

(a) Time histories of Total entropy conservation error

(b) Pressure error distribution of phase 1 at $t = 1$

(c) Pressure error distribution of phase 2 at $t = 1$

Figure 1: Results of 1D volume fraction and density wave advection test. Red: Proposed; Green: NIE; Blue: IE-H; Black dotted line: the exact analytical solution.

the ideal-gas EoS for both phases. In this study, we consider this test case with a realistic liquid-gas density ratio and appropriate stiffened-gas EoS parameters. The initial conditions are set:

$$
\begin{aligned}
&\phi_1 = \frac{1}{2} + \left(\frac{1}{2} - \phi_{\min}\right) \tanh\left(\frac{|x-\pi| - L}{2\Delta x}\right), \\
&\rho_1 = \rho_{01}, \\
&\rho_2 = \rho_{02}, \\
&u_1 = u_2 = M_0 \sin x \cos y \cos z, \\
&v_1 = v_2 = -M_0 \cos x \sin y \cos z, \\
&w_1 = w_2 = 0, \\
&p_1 = p_2 = p_0 + \frac{\rho_0 M_0^2}{16} (\cos 2x + \cos 2y)(\cos 2z + 2).
\end{aligned}
\tag{61}
$$

where p_0 is the reference pressure, and ρ_0 is the initial mixture density defined by $\rho_0 = \phi_1\rho_{01} + \phi_2\rho_{02}$. We set the initial Mach number $M_0 = 0.4$, and the reference pressure is set to $p_0 = 1000$ considering that the scale of dynamic pressure of the liquid phase is around $\rho_{01}M_0^2 \approx 160$. The length scale L is chosen to be 1, and the offset value of the volume fraction $\phi_{\min}$ is set to 10^{-6}. The computational domain is a three-dimensional periodic box $[0, 2\pi]^3$ discretized with 64^3 equidistant grid points. In this test, we solve the full seven-equation model coupled with phase-field method. The parameters for the phase-field method are set to $\Gamma = |\vec{u}_k|_{\max}$ and $\epsilon = \Delta x$, where $|\cdot|_{\max}$ denotes the maximum value of phase k in the computational domain.

Figure 2 shows snapshots of the interfaces and vortical structures. At $M_0 t = 0$, the liquid phase is surrounded by the gas phase. As time progresses, the interfaces undergo complex deformation through interaction with the vortical structures.

In this test case, we evaluate the entropy-conservation error associated with the conservative convection and regularization terms, denoted by $\langle \rho s \rangle^{\text{error}}$, after subtracting the entropy production due to the non-conservative and source terms from the total entropy ρs. Figure 3 shows the time histories of $\langle \rho s \rangle^{\text{error}}$. IE-H diverges immediately, whereas both the proposed scheme and NIE remain stable and conserve entropy at the discrete level. A magnified view reveals that the proposed scheme exhibits better entropy-conservation property than NIE.

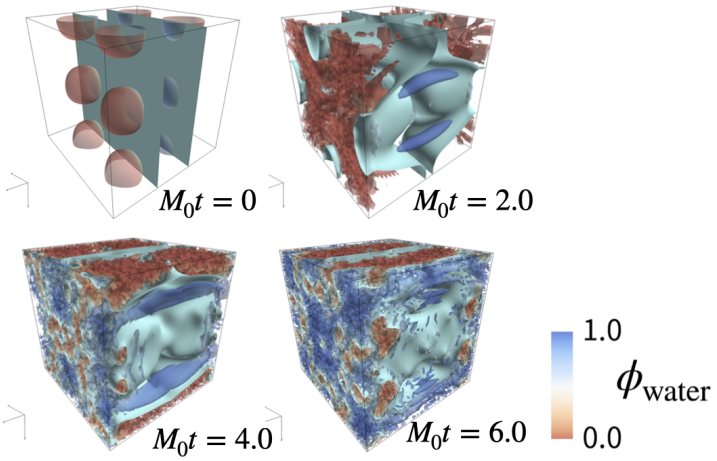

Figure 2: Snapshots of the 3D inviscid two-phase Taylor–Green vortex problem with the proposed scheme. The solid surface represents the interface (iso-surface of $\phi_1 = 0.5$), and the translucent surface represents an iso-surface of Q-criterion colored by the volume fraction of water.

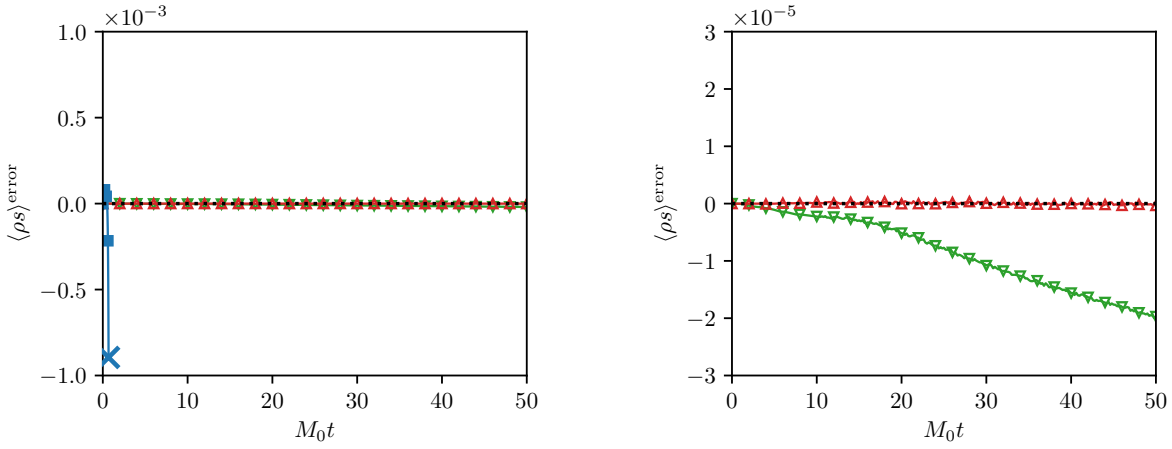

(a) Overview

(b) Close up view for NIE, IE-H

Figure 3: Time histories of the total entropy conservation error in the 3D inviscid Taylor–Green vortex test. Lines as in Fig. 1.

5. Conclusion

In this study, we developed non-dissipative and robust scheme for compressible two-phase flows. We employ the seven-equation model and stiffened-gas equation of state for the governing equations, and derived the numerical formulations that satisfy three key properties: Kinetic energy and entropy conservation, the interface equilibrium condition, and the consistency with interface-capturing method. The numerical tests demonstrated that the proposed scheme achieves strict entropy conservation and enables robust simulations of compressible two-phase flows, even under realistic liquid-gas scenarios. For further details, the reader is referred to Ref. [10].

Acknowledgements

This work was supported in part by JSPS KAKENHI Grant Number 25K01413.

References

[1] E. Tadmor. The numerical viscosity of entropy stable schemes for systems of conservation laws. I. *Mathematics of Computation*, 49:91–103, 1987.
[2] F. Ismail and P. L. Roe. Affordable, entropy-consistent Euler flux functions II: Entropy production at shocks. *Journal of Computational Physics*, 228:5410–5436, 2009.
[3] P. Chandrashekar. Kinetic energy preserving and entropy stable finite volume schemes for compressible Euler and Navier-Stokes equations. *Communications in Computational Physics*, 14:1252–1286, 2013.
[4] H. Ranocha. Comparison of some entropy conservative numerical fluxes for the Euler equations. *Journal of Scientific Computing*, 76:216–242, 2018.
[5] Y. Kuya, K. Totani, and S. Kawai. Kinetic energy and entropy preserving schemes for compressible flows by split convective forms. *Journal of Computational Physics*, 375:823–853, 2018.
[6] M. R. Baer and J. W. Nunziato. A two-phase mixture theory for the deflagration-to-detonation transition (DDT) in reactive granular materials. *International journal of multiphase flow*, 12:861–889, 1986.
[7] P.H. Chiu and Y. T. Lin. A conservative phase field method for solving incompressible two-phase flows. *Journal of Computational Physics*, 230(1):185–204, 2011.
[8] S. Mirjalili, C.B. Ivey, and A. Mani. A conservative diffuse interface method for two-phase flows with provable boundedness properties. *Journal of Computational Physics*, 401:109006, 2020.
[9] S. S. Jain, A. Mani, and P. Moin. A conservative diffuse-interface method for compressible two-phase flows. *Journal of Computational Physics*, 418:109606, 2020.
[10] S. Yoshida, S. Kawai, and S. Kawai. Kinetic energy and entropy preserving (KEEP) scheme for compressible two-phase flows with seven equation model. (To be submitted).
[11] R. Saurel and R. Abgrall. A multiphase Godunov method for compressible multifluid and multiphase flows. *Journal of Computational Physics*, 150:425–467, 1999.
[12] R. Saurel, S. Gavrilyuk, and F. Renaud. A multiphase model with internal degrees of freedom: application to shock–bubble interaction. *Journal of Fluid Mechanics*, 495:283–321, 2003.
[13] R. Saurel and C. Pantano. Diffuse-interface capturing methods for compressible two-phase flows. *Annual Review of Fluid Mechanics*, 50:105–130, 2018.
[14] D. Furfaro and R. Saurel. A simple HLLC-type Riemann solver for compressible non-equilibrium two-phase flows. *Computers & Fluids*, 111:159–178, 2015.
[15] S. S. Jain and P. Moin. A kinetic energy–and entropy-preserving scheme for compressible two-phase flows. *Journal of Computational Physics*, 464:111307, 2022.
[16] L. H. Hatashita and S. S. Jain. Interface Preservation in Modeling Compressible Two-Phase Flows Using Six-and Seven-Equation Formulations. In *AIAA SCITECH 2025 Forum*, page 1881, 2025.
[17] R. Abgrall. How to prevent pressure oscillations in multicomponent flow calculations: a quasi

conservative approach. *Journal of Computational Physics*, 125(1):150–160, 1996.

[18] Y. Tamaki, Y. Kuya, and S. Kawai. Comprehensive analysis of entropy conservation property of non-dissipative schemes for compressible flows: KEEP scheme redefined. *Journal of Computational Physics*, 468:111494, 2022.

[19] C. De Michele and G. Coppola. Numerical treatment of the energy equation in compressible flows simulations. *Computers & Fluids*, 250:105709, 2023.

[20] S. Kawai and S. Kawai. Logarithmic mean approximation in improving entropy conservation in KEEP scheme with pressure equilibrium preservation property for compressible flows. *Journal of Computational physics*, 530:113897, 2025.

[21] N. Shima, Y. Kuya, Y. Tamaki, and S. Kawai. Preventing spurious pressure oscillations in split convective form discretization for compressible flows. *Journal of Computational Physics*, 427:110060, 2021.